

## TiO<sub>2</sub> Nanoparticles in Bulk Heterojunction P3HT-PCBM Organic Solar Cell

Kamlesh Kukreti<sup>1\*</sup>, Arun Pratap Singh Rathod<sup>2</sup>, Brijesh Kumar<sup>3</sup>

<sup>1,2</sup>Department of Electronics and Communication Engineering  
Graphic Era University, Dehradun, India

<sup>3</sup>Department of Electronics and Communication Engineering  
Madan Mohan Malaviya University of Technology, Gorakhpur, India

kamlesh.kukreti23@gmail.com, major.rathod@gmail.com, brijesh\_ece@mmmut.ac.in

\*Corresponding author

(Received March 4, 2016; Accepted July 1, 2016)

### Abstract

This research paper aims to present a concise, depth insight of organic solar cells. Subsequently, this paper also discusses various recent advancements in organic solar cells in terms of material, structures and other performance influencing factors. This paper reviewed to see the effect of TiO<sub>2</sub> nano particles on  $\eta$  in the BHJ polymeric solar cell by its incorporation into the composite active (photovoltaic) layer, comprised of poly3-hexyl-thiophene P3HT, and [6,6]-phenylC<sub>61</sub>-butyricacid-methylester (PCBM). Nano-structured TiO<sub>2</sub> exhibits good processability, favourable characteristics of the transport of electrons, and brilliant physical as well as chemical stability which are important wants in solar cells as impact of blending of TiO<sub>2</sub> nano particles in between photo-active layers is elucidated the electrical performance of P3HT-PCBM- based solar cells. This paper relates to bulk heterojunction organic solar cells. More specifically, the enhancement of PCE of solar cell based on polymer, using mix of poly 3-hexylthio-phene(P3HT), derivatives of C<sub>60</sub> as [6, 6]-phenyl C<sub>61</sub>butyric-acidmethylester (PCBM) and TiO<sub>2</sub> nano particles has been reported. P3HT-TiO<sub>2</sub> based solar cell has also been fabricated as there is a probability of improvement in  $\eta$  and J<sub>SC</sub> by optimizing the blending concentration of TiO<sub>2</sub> nano particles.

**Keywords-** PCBM ([6, 6]-phenyl C<sub>61</sub>butyric Acid-Methyl Ester), P3HT (Poly (3-hexylthiophene)), TiO<sub>2</sub> (Titanium Dioxide), PCE (Power Conversion Efficiency), BHJ (Bulk Heterojunction).

### 1. Introduction

The inorganic solar cell has high costs imposed on fabrication which makes it suitable for limited use, (Coakley and Mcgehee, 2004) as measures involving high temperature upto (400°C-1400°C), high vacuum, and several lithographic steps. An organic solar cells can be used as low alternative includes the use of polymers or small molecules having power efficiencies up to 5% whereas conventional inorganic solar cells reveal solar efficiencies up to 10% but also the models having large cost can reach efficiency upto 40%.

Solar cell based on polymer thin films, are to be spin-coated or can be printed over transparent substrates to provides an another idea to the conventional inorganic solar cells with potential advantages having less costly, easy to built-up, and light weight (Braun, 1984).

Earlier, the (PCE) conversion efficiency of polymer based solar-cells has been gradually enhanced as improvement in development of device architectures (Shockley and Queisser, 1961). However, the inadequate utilization of the incident sun light remains one of the major limitations on the valuable and consistent operation in organic solar cells. Here, the problem can be solved by studying the various parameters by using so called bulk heterojunction (BHJs) (Green, 1982) or by changing the thickness of the photoactive layer respectively.

In this paper, utilizing of  $\text{TiO}_2$  and its effects has been seen over PCE (Power Conversion Efficiency) in BHJ solar cell based on polymer by introducing titanium dioxide nano particles into the composite photo-active layer, composed of P3HT and PCBM. Nano structured  $\text{TiO}_2$  shows good transport characteristics of electron, high processability and excellent physical as well as chemical stability which are significant, necessities in the fabrication of plastic transparent solar cells. The influence of  $\text{TiO}_2$  nano particles in active layers P3HT-PCBM is elucidated on electrical performance of based organic solar cells. The series resistance has been reduced and also increases in open circuit voltage on increasing the concentration of  $\text{TiO}_2$  nano particle. Furthermore, the higher refractive index of  $\text{TiO}_2$  increases the probability of trapping the light energy into the P3HT-PCBM of active-layer based solar cell.

## 2. Literature Survey

The organic semiconductor has the potential to create some devices which are economically and reliable, furthermore generate power with unlimited availability of organic material. Organic semiconductors can be considered as environmentally safe having low cost and is another option to inorganic semiconductors such as Si as they are having elevated optical absorption-coefficients which provide probability for manufacturing of thin film solar-cells. Low temperature approaches are well recognized for roll to roll processes for printing techniques (Brabec, 2004; Choong et al., 1996; Kallmann and Pope, 1959). This particular probability of utilizing thin flexible substrates made up of thin plastics in a printing process as it can be done easily which decreases balancing cost for organic solar cell (Chapin et al., 1954). The organic semiconductors materials composed based on conjugated  $\pi$  - electrons. A variation between singly and, double carbon - carbon bonds defines conjugated organic method. Single bonds i.e  $\sigma$ -bond is directly related with localized double bonds, electrons consist of a one  $\sigma$  bond and one  $\pi$  bond. The  $\pi$  electrons can jump from one site to other site as they are smaller than the  $\sigma$ -electron between carbon atoms. Furthermore, the overlapping of  $\pi$ -orbitals mutually within, the conjugation-path can delocalize the functions of wave all over the conjugated backbone. The  $\pi$  band which is empty known as LUMO (Lowest Unoccupied Molecular Orbital) or with electrons known as HOMO (Highest Occupied Molecular Orbital). The band gap of organic material lies between 1-4 eV. Examples of conjugated organic materials are there in Figure 1.

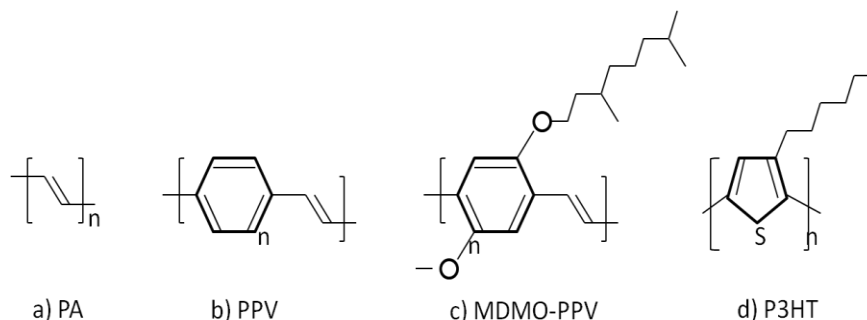


**Figure 1. Dual Chemical structure and abbreviation few conjugated organic molecules. Left: poly-(acetylene) PA, poly para-phenylene- (vinylene) PPV, a substituted PPV ( MDMO-PPV ) and pol (3-hexyl thio-phen) P3HT [Barth S. & B"assler H. (1997)]**

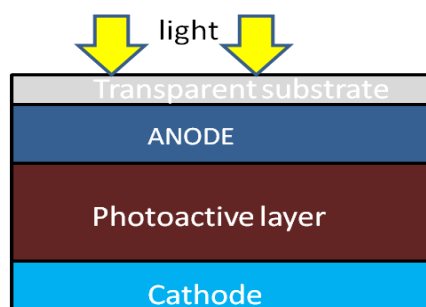


**Figure 2. Schematic layout of an organic solar cell**

In this an organic solar cell contains of a photo-active layer sandwiched between two same or may be different electrodes layer, from which one should be translucent which permit the photons to reach photo-active layer, in Figure 2. This photo-active layer can be single, bilayer, or can be blend of two or more components (Granstrom et al., 1998). The charge was originated at the interface on the photo-active layer on absorption of sunlight hence, electric field is generated, provided as per the irregular ionization energies, of the electrodes and these carrier charges are transported as well as collected at the load. Hence, organic solar-cell transforms light energy into electricity. The reported organic solar cell, firstly came in 1959, when an anthra-cene crystal was considered. This cell is having low efficiency and consists of photovoltage of 200 mV (Da Costa and Conwell, 1993; Marks et al., 1994). Furthermore, tremendous increase in the research of organic solar cell devices based on single layer organic materials in which efficiencies is below 0.1%, making it inappropriate for any applications. Primarily, due to the absorption of solar energy in the form of photons in organic materials resulting creation of a charge carrier known to as exciton, as free hole electrons pairs as generated in inorganic solar cells as organic semiconductors are defines or characterizes by low dielectric constant, as compared as inorganic semiconductors, which requires an energies greater than the thermal energy (kT) for dissociating excitons (Barth and Bassler, 1997). The electric field generates at the electrodes were not sufficient for breaking these photo-generated excitons as an alternative, the excitons diffuses at the interface of organic layer as they arrive at the electrodes, they dissociate to distribute separate charges or, may be recombine while the diffusion lengths of exciton should be 1 to 10 nm (Tang, 1986;

Grätzel, 2001; O’regan and Grätzel, 1991; Jana, 2000; Peumans et al., 2000) as than the device thicknesses being much larger than diffusion length, the diffusion length of excitons confines generation of charge carrier in these devices, since most of excitons were lost when recombination takes place time (Gregg, 1996). Hence, photo-generation is a process of the available for dissociation of exciton. A most important benchmark in organic solar cell performances reported in 1986 when, Tang revealed greater efficiencies of about 1% are possible when combining a donor and an acceptor together, in one structure.

## 2.1 Principle Operation of Bulk Heterojunction OSC

Most important development that has enhanced the output characteristics of organic solar cell are basically D/A hetero-junctions’ devices. The bulk heterojunction based devices is to uses mixture of two organic materials having different electron affinities, and ionization potentials (Granstrom et al., 1998). The output potential should be well-built and support excitons and dissociation takes place at the interface, the electrons will be absorb by the organic material having greater electron affinity and the holes having smaller ionization potential, provided that the potential difference should be greater than, the binding energy of exciton (Halls et al., 1995). In planar heterojunction or ‘bilayer’ device, the organic D/A interface distributes excitons efficiently as compared to an organic/metal, interface in the single-layer devices.

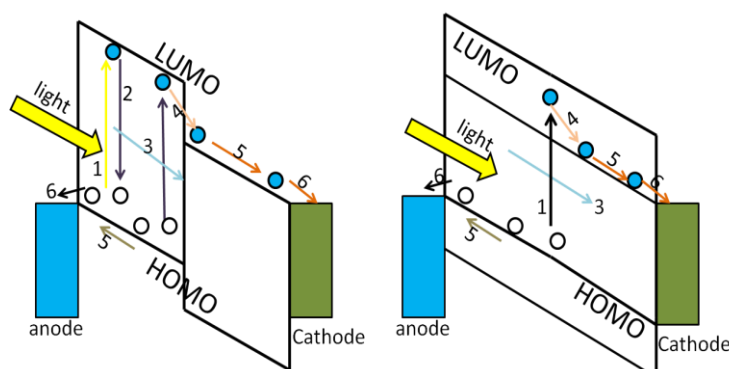
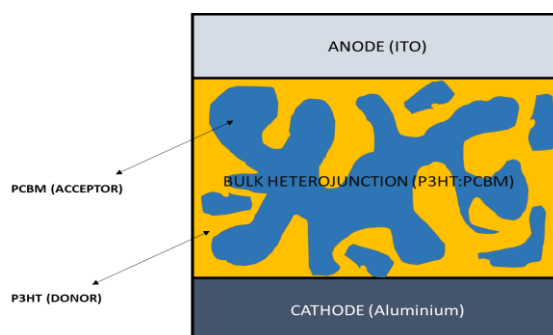


Figure 3. The energy diagram of a bilayer device

The energy diagram of a bilayer device is shown in the Figure 3. Sun-light in the form of photons is traced inside the device interface (1), which leads to the development of excitons at the donor material. However, n type material known as acceptor, also absorb photons but for the ease, the donor phase is considered for the absorption. The developed excitons then started to diffuse (3) at the donor, phase as excitons come upon at the interface within the acceptor then dissociation takes place (4) resulting separation of charges. The design and synthesis of polymers and can be casted using techniques such as, spin coating, screen printing which represent attractive route for large scale production of organic solar cell consisting flexible transparent, substrates. Therefore, photo-induced electron transfers, from a polymer as Buckminster-fullerene ( $C_{60}$ ) or its derivatives as acceptors, this was reported by (Brabec et al., 2001). In year 1995, (Yu et al., 1995) fabricated bulk heterojunction consist of blend of PPV and fullerene derivative (PCBM) that acts as an acceptor resulting power

efficiencies of 5%. Figure 1 (d) as absorbing as well as electron donating material. The hole-electrons pairs across the A/D interface may still recombine and, electric field is required to separate them into free charges (Ghosh and Feng, 1978; Law, 1993). Subsequently, the separated free charges i.e. holes are to be transported (5) and collected towards the anode as electrodes have different work function (6). Furthermore, decay of excitons (2) yielding, if they are to be generated far-off from its interface. Hence, excitons should be formed up to its diffusion length at the interface; if exciton diffusion length is equal to the length scale of the mixture then decay of exciton (2) will be reduced.



**Figure 4. The schematic layout of bulk heterojunction organic solar cell**

The bulk hetero-junction is the major powerful concept nowadays for all, organic solar cells as shown in Figure 4. In 1990s, Gratzel reported Dye-sensitized solar cells, however, works on same principles. The organic materials which uses as photo-active layer in bulk hetero-junction solar cells that have got tremendous attention in the last few years are semi-conducting polymers as well as small-molecules (Padinger et al., 2003; Brabec et al., 2001). They consist of optoelectronic properties with the mechanical properties and excellent processing of conventional semiconductor material. Furthermore, they consist of a unique flexibility in, permitting for variation to the broad range of properties such, as bandgap, energy levels, structural and wetting properties as well as doping.

## **2.2 Hybrid Bulk Heterojunction (P3HT-PCBM-TiO<sub>2</sub>)**

Here the discussion is about seeing the effect of TiO<sub>2</sub> nanoparticles on  $\eta$  in the Bulk heterojunction polymeric solar-cell by its incorporation into the composite active (photovoltaic) layer, composed of poly (3-hexylthio-phenylene) (P3HT) and [6,6]-phenylC<sub>61</sub>-butyric acid methyl ester (PCBM). Nano-structured TiO<sub>2</sub> exhibits high process abilities, favorable transport characteristics of electron and excellent physical as well as chemical properties, which are major need in fabrication of plastic based solar cells. This material enables the controllable patterning of a bulk heterostructure on the micro-to-nano scale, thereby providing a large contact interface with nearby organic molecules. The blending of TiO<sub>2</sub> nano-particles in photoactive layer is elucidated on the electrical properties of P3HT-PCBM-based organic solar cells (Chirvase et al., 2004; Kim et al., 2005).

The entire structure is described as glass/indium tin-oxide (ITO)/ (PEDOT: PSS,)/ P3HT-PCBM-TiO<sub>2</sub>/Ca/Al. This suggests that the optical feature of the active layer (P3HT-PCBM blend) is not changed by inserting an inactive do pant material. The existence of TiO<sub>2</sub> nanoparticles does not inhibit the diffusion of light throughout the film. The spectra obtained in reflectance mode, through 60 mg/ml concentration, yield more interesting information as illustrated in Figure 5. The reflectance of the reference sample, which is a purely polymeric cell, is low (similar to 10%) in the UV/Vis range, where the intrinsic absorption of the P3HT-PCBM blend is dominant.

The spectral features of reflection in this range are approximately inversely proportional to the shape of the basic absorption bands of the polymer film, except at  $\lambda < 280$  nm, where the contribution of the anode materials become prominent. However, at wavelengths of over 630 nm, reflection becomes notably more pronounced (more than 50%) and reaches a maximum of 68% in the near infrared, at approximately 950 nm as shown in Figure 5.

The red part of the spectrum is complex, and warrants further investigation. Notably, the spectral activity of materials used in solar cells in the near infrared domain is often obscured, although the photovoltaic response to solar illumination herein may have increased the efficiency of the device (Green et al., 2005). The reflectance spectrum of P3HT-PCBM-TiO<sub>2</sub> nanocomposite cells differs markedly from that of the undoped device. As shown in Figure 5, in the UV/Vis range, the reflectance, again, is controlled by the intrinsic P3HT-PCBM absorption, whilst in the near infrared, reflectance remains low, at about 10%, which is in contrast with that of the reference cell. It is believed that this low reflectance is one of the reasons (the “optical” reason) for the higher  $\eta$  value of the devices herein.

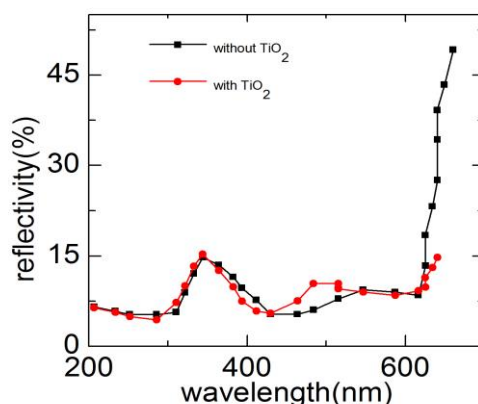


**Figure 5. Reflectance spectra from glass/ITO side of reference cell and cell with 5.0% TiO<sub>2</sub> nanoparticles. The inset shows the images of P3HT-PCBM films on the glass substrate without and with 5.0% TiO<sub>2</sub> nanoparticles**

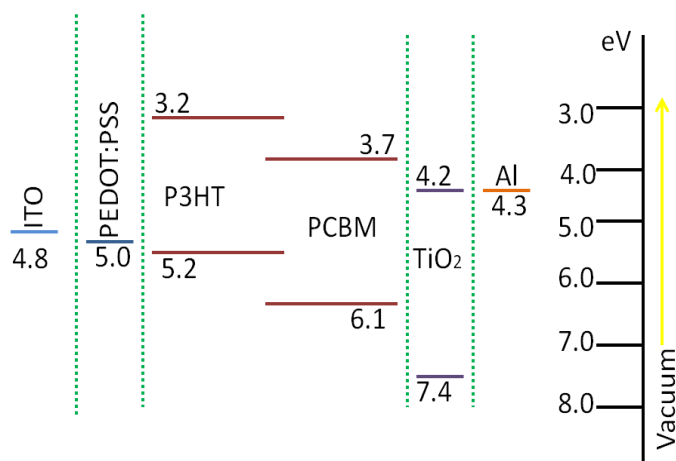


**Figure 6.** A schematic showing the energy levels of materials used in the device

Another (“electrical”) reason involves the optimization of the electron collecting process at the electrode/polymer interface by the introduction of TiO<sub>2</sub>. Figure 6 shows the relative positions of the energy levels according to data obtained from elsewhere. Indeed, based on the possible interactions between the hydrophobic P3HT side chains and the hydrophilic TiO<sub>2</sub> surface, during the formation of the composite films, most of the nanoparticles are forced to the topmost polymer layer, where they may further combine. Represents output characteristics of cylindrical OTFT calculated by analytical modeling and verifying the mathematical model of the organic transistor.

### 3. Motivation

Digital as the worldwide, demand in energy continuously increases every year rapidly, the decrease in distributing non-renewable sources of energy such as coal, oil and uranium and their long term dangerous effects on nature of our planet, includes to give emphasis to the necessity to develop renewable sources of energy. Here, plants are not able to trap the enormous quantity of more CO<sub>2</sub> out in earth’s atmosphere mainly, due to burning of fossil - fuels. Further, the enhanced concentration of CO<sub>2</sub> in the atmosphere significantly increases up to the greenhouse effect which is responsible for global warming (Goetzberger et al., 2003). The consequences of these probabilities are already seen by increasing harshness of natural disasters. Fortunately, sources of energy that are renewable which may or not having any significant damaging effects on the nature. Tracing sun-light energy directly, from sun by using photo-voltaic technology is generally known as an important component for future production of energy worldwide. Organic solar cell devices can be made economically as well as competitive with other emerging technologies which should be related to renewable energy, large extent of manufacturing of organic solar cell devices includes a sustainable energy, source which provides an important proportion of energy which we use daily. The solar cells devices have broadly studied since the 1960s, at Bell Laboratories first crystalline, solar-cell based on silicon was developed which have an efficiency of 6% (Goetzberger et al., 2003). Since then, there has been a tremendous effort in the field of the solar cell as

efficiency reached, 24% for crystalline Si based solar cells, and also close to the speculative predicted efficiency of 40%.

#### **4. Research Methods**

Digital to characterize the devices, several measurements were performed. These include:

- 4.1 Absorption spectrum measurement.
- 4.2 Reflection spectrum measurement.
- 4.3 I-V measurements.
- 4.4 X-ray diffraction.
- 4.5 Thickness measurement.
- 4.6 Surface roughness measurement.

##### **4.1 Absorption Spectrum**

The absorption spectrum of the polymer-fullerene and polymer-fullerene-titanium blend in thin film form was obtained using Lambda 750 spectrophotometer. The wavelength of the incident light was varied from 300 nm to 900 nm.

##### **4.2 Reflection Spectrum**

The reflection spectrum of the polymer-fullerene and polymer-fullerene-titanium dioxide blend in thin film form was obtained Lambda 750 spectrophotometer. The wavelength of the incident light was varied from 300 nm to 900 nm.

##### **4.3 I-V Measurements**

The measurements should be taken through solar simulator. This is a light source, are capable specially to simulate solar radiations known as solar simulators. They produce a parallel and uniform output beam with spectral match which is close to sun light. We provide several other types with different spectra and irradiance output, depending on the size of beam and air mass filters used. We can use xenon arc lamps as a radiation source because of the reason that they provide the closest spectral match to the solar spectrum may be available from any commercial source.

To characterize at 1 sun ( $100\text{mW}/\text{cm}^2$ ) a solar simulator from Newport Corporation was used. The spectrum of the simulator is shown in Figure 7 (Verploegen et al., 2010).



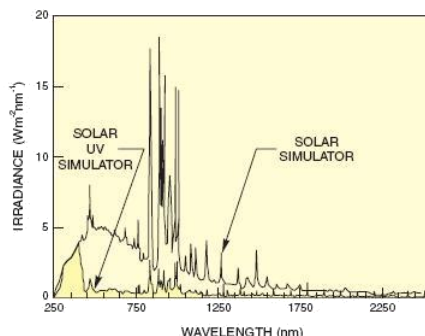


Figure 7. Spectrum of the solar simulator used for characterization [Verploegen Eric (2010)]

#### 4.4 X-Ray Diffraction (XRD)

XRD patterns are obtained by the instrument Rich-Seifert X-ray diffractometer (model Isodebyeflex2002) using, Cu K $\alpha$  ( $\lambda = 1.540598\text{\AA}$ ). This helps to find out the phases present in the sample, crystallinity and also the particle size by knowing the orientation of the planes by comparing the XRD pattern obtained with the standard data available. The calcined powder has been taken on a glass plate and makes it uniform throughout with the help of another glass plate, add ethyl alcohol to wet the sample and dry it. The surface gets uniform such that the X-rays can incident and reflected back from a uniform surface.

The XRD is done from 20° to 70° since the peaks are expected to be in between these values. The  $R_{XRD}$  was calculated from the Full Width at Half Maximum (FWHM) of the most intense peak using Scherer's equation.

$$R_{XRD} = \frac{0.9 * \lambda}{B * \cos \theta} \tag{1}$$

Where,  $\lambda$  is the wavelength of Cu K $\alpha$  line of value 1.541841 $\text{\AA}$ , B is Full Width Half Maximum in radians (FWHM) and  $2\theta$  is the angle corresponding to the maximum intensity in the XRD plot.

#### 4.5 Thickness Measurement

Thickness measurement is done on profilometer ( $\alpha$ -stepper). A tip of diamond with calibrated force of contact is bringing into the, direct contact within the surface. The motion of the tip is amplified detected and filtered as the tip move across the surface. Major measurement factors are: tip radius, 0.1 micron (in grating-dispersion direction), digital sampling 2 kHz, 5 microns/sec tip speed, 0.25 milli-gram tipforce, and profile length of at least 100 microns. The sample is placed on the platform and the scan length and scan speed is selected. The stylus scans the given length and the step gives the thickness of the deposited layer.

#### 4.6 Surface Roughness Measurements

The (AFM) Atomic Force Microscope or (SFM) Scanning Force Microscope is a high-resolution of scanning, probe microscope which can be demonstrated as a resolution of, fractions of a nanometer (nm), which is 1000 times superior than the optical diffraction limit.

### 5. Results and Analysis

#### 5.1 Electrical Properties

These Bulk Heterojunction Devices of P3HT-PCBM & P3HT-PCBM-TiO<sub>2</sub>. In this experiment, P3HT-PCBM and P3HT-PCBM-TiO<sub>2</sub> bulk heterojunction, device were made within active layer thicknesses of 70nm. P3HT-PCBM and P3HT-PCBM-TiO<sub>2</sub> solution was made in Chloro-benzene solvent with a concentration, of 20 mg/ml. The device structure contains of the following layers as shown in Figure 8.

An organic solar cell consists of a photo-active layer between two electrodes made up of different material, anode should be transparent in, order to permit the received photons to reach the photo-active layer. Here this photo-active layer is made by mixing of two (or more) components.

Upon absorption of light, the charge carrier that originates at the interface of photo-active layer and due to which electric field is generated provided, by the irregular ionization energies of the electrodes as these charges are transferred and collected in the external circuit. Hence there is a process of an organic solar-cell which converts, light into electricity.

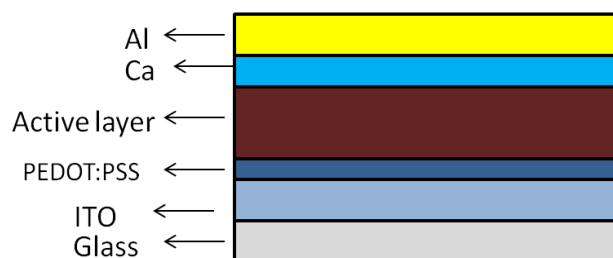
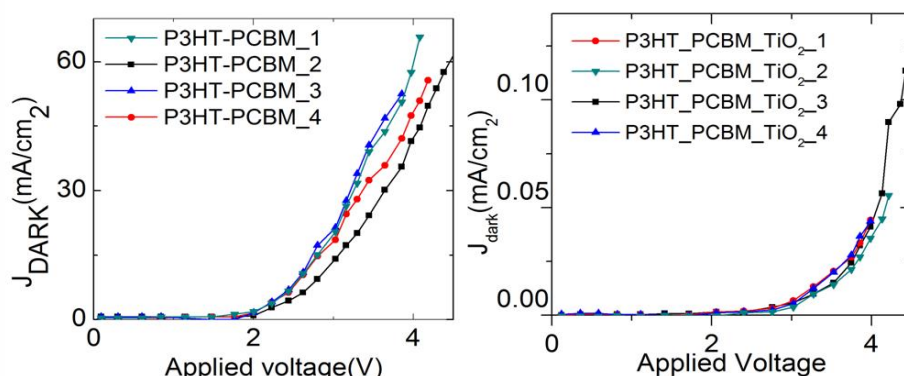


Figure 8. Device structure

Here, (P3HT-PCBM and P3HT-PCBM-TiO<sub>2</sub>) based devices have been fabricated with active layer thickness of 70 nm with P3HT-PCBM (1:1) and P3HT-PCBM-TiO<sub>2</sub> (1:1:0.075). TiO<sub>2</sub> has been added in P3HT-PCBM with weight percentage (<5%), so that it can show, its effect. Solutions were made in chlorobenzene solvent with a concentration of 20 mg/ml with 1000 rpm, 60 seconds spin speed. Thickness of PEDOT: PSS thickness is 120 nm. Thickness of Calcium is 40 Å and that of aluminum is 700 Å.



**Figure 9. Linear J-V characteristic of P3HT-PCBM and, P3HT-PCBM-TiO<sub>2</sub> device under dark**

In forward bias we have both the injected carriers and photo generated carriers. In Figure 9 device P3HT-PCBM exhibits a short circuit current density ( $J_{sc}$ )  $162 \mu\text{A}/\text{cm}^2$ , open circuit voltage of 0.58 volt, and fill factor value 0.15 at 1 sun light illumination. Device P3HT-PCBM-TiO<sub>2</sub> exhibits a short circuit current density ( $J_{sc}$ )  $1.89 \mu\text{A}/\text{cm}^2$ ,  $V_{OC}$  of 1.18 volt, and fill factor value 0.08 at 1 sun light illumination. Built in voltage for P3HT-PCBM is 0.50 V and P3HT-PCBM-TiO<sub>2</sub> is 0.90V.

Higher  $V_{OC}$  in P3HT-PCBM-TiO<sub>2</sub> may be due to the higher shunt resistance provided by TiO<sub>2</sub> nanoparticles. The maximum limit of open circuit voltage in case of P3HT-PCBM is 1.5 V and P3HT-PCBM-TiO<sub>2</sub> is 1.0 volts.

In this case, solar cell having TiO<sub>2</sub> nanoparticles maximum  $V_{OC}$  found to be 1.23V, which means that electrode effect is coming into picture and the maximum  $V_{OC}$  is governed by difference of electrode work function (2.2 V in this case).

Figure 10 shows the characteristic in dark in semi log scale. It is clear that On-Off ratio for P3HT-PCBM-TiO<sub>2</sub> is more than P3HT-PCBM as shown in Figure 10.

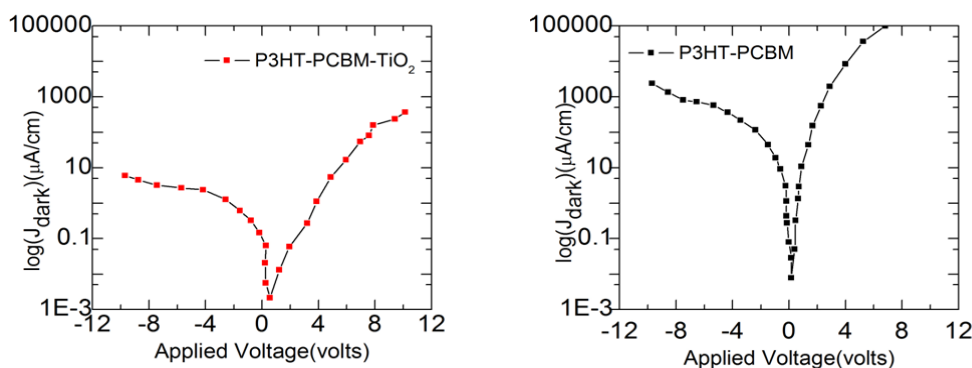


**Figure 10. J-V characteristic in semi-log scale under dark for P3HT-PCBM and P3HT-PCBM-TiO<sub>2</sub>**

ON-OFF Ratio	P3HT-PCBM-TiO <sub>2</sub>	P3HT-PCBM
+/-10V	102	73

**Table 1. ON-OFF ratio for P3HT-PCBM, and P3HT-PCBM- TiO<sub>2</sub>**

Device	V bi ( Volts)
P3HT-PCBM	0.50
P3HT-PCBM-TiO <sub>2</sub>	0.90

**Table 2. Built in voltage for P3HT-PCBM and P3HT-PCBM-TiO<sub>2</sub>**

Table 1 shows that On-Off ratio is more as it TiO<sub>2</sub> helps in injection. One possible reason behind higher built in voltage and lower short circuit current in P3HT-PCBM-TiO<sub>2</sub> can be the TiO<sub>2</sub> nanoparticles behaving as bulk shown in Table 2, which is due to bad dispersion of TiO<sub>2</sub> nanoparticles throughout active layer or small active layer thickness in comparison of TiO<sub>2</sub> nanoparticles sizes. Figure 11 shows the characteristic in dark in log-log scale.

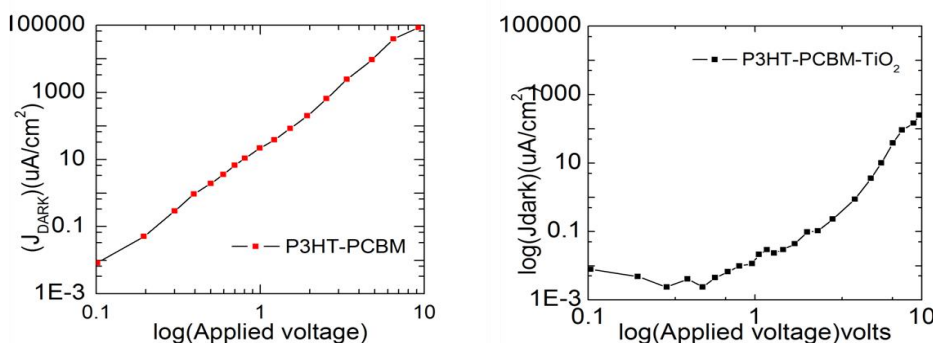


**Figure 11. J-V characteristic in log-log scale for P3HT-PCBM and P3HT-PCBM-TiO<sub>2</sub>**

In case of P3HT-PCBM, slope of the trap filling region is less as compare to P3HT-PCBM-TiO<sub>2</sub> devices, which shows that trap distribution is gradual (extended) in P3HT-PCBM and abrupt distribution of traps in P3HT-PCBM-TiO<sub>2</sub>. The possible reason behind later can be rough film formation in TiO<sub>2</sub> nanoparticles case. In other words, it can be referred that P3HT-PCBM-TiO<sub>2</sub> has more number of traps as at the same voltage it has less current.

## 5.2 Efficiency Calculation

Devices show solar cell characteristics with changes in open circuit voltage (VOC), short circuit current density (JSC) and Fill Factor (FF). Photovoltaic parameters of P3HT-PCBM and P3HT-PCBM-TiO<sub>2</sub> has been tabulated in Table 3.

P3HT-PCBM				P3HT-PCBM-TiO <sub>2</sub>			
V <sub>oc</sub> (Volts)	J <sub>sc</sub> (μA/cm <sup>2</sup> )	Fill Factor	η (%)	V <sub>oc</sub> (Volts)	J <sub>sc</sub> (μA/cm <sup>2</sup> )	Fill Factor	η (%)
0.575	162.08	0.15	0.072	1.18	1.89	0.08	0.0008
0.575	127.14	0.15	0.056	1.15	1.52	0.07	0.0008
0.575	165.74	0.15	0.069	1.23	1.44	0.07	0.0007
0.549	116.98	0.14			0.87		
			0.049	1.00		0.08	0.0004

**Table 3. Parameters of P3HT-PCBM and P3HT-PCBM-TiO<sub>2</sub>**

## 6. Conclusion

In this paper reviewed to see the effect of TiO<sub>2</sub> nanoparticles on η in the polymeric bulk heterojunction solar cell by its incorporation into composite active layer, comprises of poly (3-hexylthio-phen) (P3-HT) and 6, 6-phenylC<sub>61</sub>butyric-acidmethylester (PCBM). Nano-structured TiO<sub>2</sub> exhibits elevated processability, favourable characteristics of electron, and excellent physical and chemical properties, which are major need in solar cells. The influence of mixture TiO<sub>2</sub> nanoparticles in photo-active layers is elucidated the electrical performance of P3HT-PCBM-based organic solar cells. This paper relates to bulk heterojunction organic solar cells. More specifically, in this paper, the enhancement in (PCE) Power Conversion Efficiency of polymer based solar cell using mixture of film of poly 3-hexylthio-phen (P3HT), derivatives of C<sub>60</sub> 6,6-phenyl C<sub>61</sub>-butyricacid-methylester (PCBM) and TiO<sub>2</sub> nanoparticles has been reported. P3HT-TiO<sub>2</sub> based solar cell has also been fabricated as there is a probability of improvement in η and J<sub>sc</sub> by optimizing the blending concentration of TiO<sub>2</sub> nano particles device.

## References

- Barth S., & Bassler, H. (1997). Intrinsic photoconduction in PPV-type conjugated polymers. *Physical Review Letters*, 79(22), 4445-4447.
- Brabec, C. J., Zerza, G., Cerullo, G., De Silvestri, S., Luzzati, S., Hummelen, J. C., & Sariciftci, S. (2001). Tracing photo induced electron transfer process in conjugated polymer/fullerene Bulk heterojunctions in real time. *Chemical Physics Letters*, 340(3), 232-236.
- Brabec, C. J. (2004). Organic photovoltaics: technology and market. *Solar Energy Materials and Solar Cells*, 83(2), 273-292.
- Brabec, C. J., Sariciftci, N. S., & Hummelen, J. C. (2001). Plastic solar cells. *Advanced Functional Materials*, 11(1), 15-26.
- Braun, C. L. (1984). Electric-field assisted dissociation of charge-transfer states as a mechanism of photo carrier production. *Journal of Chemical Physics*, 80(9), 4157-4161.
- Chapin, D. M., Fuller, C. S., & Pearson, G. L. (1954). A new silicon p-n junction photo cell for converting solar radiation into electrical power. *Journal of Applied Physics*, 25(5), 676-677.
- Chirvase, D., Parisi, J., Hummelen, J. C., & Dyakonov, V. (2004). Influence of nano morphology on the photo voltaic action of polymer-fullerene composites. *Nano Technology*, 15(9), 1317-1323.

- Choong, V., Park, Y., Gao, Y., Wehrmeister, T., Muellen, K., Hsieh, B. R., & Tang, C. W. (1996). Dramatic photoluminescence quenching of phenylene vinylene oligomer thin films upon sub mono layer Ca deposition. *Applied Physics Letters*, 69(10), 1492-1494.
- Coakley, K. M., & Mcgehee, M. D. (2004). Conjugated polymer photovoltaic cell. *Chemistry of Materials*, 16(23), 4533-4542.
- Da Costa, P. G., & Conwell, E. M. (1993). Excitons and the band-gap in poly (phenylene vinylene). *Physical Review*, 48(3), 26-30.
- Ghosh, A. K., & Feng, T. (1978). Merocyanine organic solar cells. *Journal of Applied Physics*, 49(12), 5982-5989.
- Goetzberger, A., Hebling, C., & Schock, H. W. (2003). Photovoltaic materials, history, status and outlook. *Materials Science and Engineering R-Reports*, 40(1), 1-46.
- Granstrom, M., Petritsch, K., Arias, A. C., Lux, A., Andersson, M. R., & Friend, R. H. (1998). Laminated fabrication of polymeric photovoltaic diodes. *Nature*, 395(6699), 257-260.
- Grätzel, M. (2001). Photo electrochemical cells, *Nature*, 414(6861), 338-344.
- Green M. A. (1982). *Solar cells - Operating principles, technology and system applications*. University of New South Wales, Sydney 1-274.
- Green, M. A., Emery, K., King, D. L., Igari, S., & Warta, W. (2005). Solar cell efficiency tables (version25). *Progress in Photovoltaic*, 13(1), 49-54.
- Gregg, B. A. (1996). Bilayer molecular solar cells on spin-coated TiO<sub>2</sub> substrates. *Chemical Physics Letters*, 258(3), 376-380.
- Halls, J. J. M., Walsh, C. A., Greenham, N. C., Marseglia, E. A., Friend, R. H., Moratti, S. C., & Holmes A. B. (1995). Efficient photodiodes from interpenetrating polymer networks. *Nature*, 376(5), 498-500.
- Jana, A. K. (2000). Solar cells based on dyes. *Journal of Photochemistry and Photobiology A-Chemistry*, 132(1), 1-17.
- Kallmann, H., & Pope, M. (1959). Photovoltaic effect in organic crystals. *Journal of Chemical Physics*, 30(2), 585-586.
- Kim, Y., Choulis, S. A., Nelson, J., Bradley, D. D. C, Cook S., & Durrant J. R. (2005). Device effect in organic solar cells with blends of regioregular poly (3-hexylthiophene) and soluble fullerene. *Applied Physics Letters*, 86(6), 1-3, 063502.
- Law, K. Y. (1993). Organic photoconductive materials: Recent trends and developments. *Chemical Reviews*, 93 (1). 449-486.
- Marks, R. N., Halls, J. J. M., Bradley, D. D. C., Friend, R. H., & Holmes, A. B. (1994). The photovoltaic response in poly (p-phenylene vinylene) thin-film devices. *Journal of Physics-Condensed Matter*, 6(7), 1379-1394.
- O'regan, B., & Grätzel, M. (1991). A low-cost, high-efficiency solar-cell based on dye-sensitized Colloidal TiO<sub>2</sub> films. *Nature*, 353(6346), 737-740.
- Padinger, F., Rittberger, R. S., & Sariciftci, N. S. (2003). Effects of postproduction treatment on plastic solar cells. *Advanced Functional Materials*, 13(1), 85-88.
- Peumans, P., Bulovic, V., & Forrest, S. R. (2000). Efficient photon harvesting at high optical intensities in ultrathin organic double-hetero structure photovoltaic diodes. *Applied Physics Letters*, 76(19), 2650-2652.

Shockley, W., & Queisser, H. J. (1961). Detailed balance limit of efficiency of p-n junction solar Cells. *Journal of Applied Physics*, 32(3), 510-519.

Tang, C. W. (1986). Two-layer organic photovoltaic cell. *Applied Physics Letters*, 48(2), 183-185.

Verploegen, E., Mondal, R., Bettinger, C. J., Sok, S., Toney, M. F., & Bao, Z. (2010). Study the effects of thermal annealing on polymer/fullerene bulk heterojunction organic cells, 20(20), 3519-3529.

Yu, G., Gao, J., Hummelen, J. C., Wudl, F., & Heeger, A. J. (1995). Polymer photovoltaic cells enhanced efficiencies via a network of internal donor-acceptor hetero junctions. *Science*, 270(5243), 1789-1791.